



# ON THE NUMERICAL ACCURACY OF A COMBINED FEM/RADIATING-SURFACE APPROACH FOR NOISE PROPAGATION IN UNBOUNDED DOMAINS

Simone Mancini, R. Jeremy Astley, Gwenael Gabard and Samuel Sinayoko  
*Institute of Sound and Vibration Research, University of Southampton, SO17 1BJ, Southampton, UK*  
*email: s.mancini@soton.ac.uk*

Michel Tournour

*Siemens Industry Software NV, Interleuvenlaan 68, 3001, Leuven, Belgium*

The focus of this study is to present the limitations of a hybrid numerical method for the prediction of sound propagation and scattering within an unbounded domain. We present a combined Finite Element Method (FEM)/Radiating-surface approach based on a Kirchhoff's integral formulation with a mean flow. This work identifies the sources of numerical error inherent to the hybrid method. A potential formulation is adopted for wave propagation and the problem is set in the frequency domain. The finite element method is applied to solve the scattering problem in presence of non-uniformities. The FEM solution, combined with a Perfectly Matched Layer (PML), is mapped on a closed surface. The Kirchhoff's radiating surface with a uniform mean flow propagates acoustic waves in free field. The problem of radiation from a monopole source and the scattering by a cylinder from the same source are presented as numerical examples by accounting for a subsonic mean flow. The accuracy in the prediction of the acoustic particle velocity is critical for the efficacy of the method. The main achievement is that the detrimental effect of the mean flow on the pollution error can be limited by applying the hybrid method. On the other hand, the integral formulation is exact only for a uniform mean flow.

---

## 1. Introduction

Sound Radiation in unbounded domains is challenging from a computational point of view. The Finite Element Method (FEM) allows predicting noise propagation in presence of non-uniformities and complex geometries. Nevertheless, it suffers from numerical dispersion and pollution [1]. These errors are amplified by the presence of a base flow [2]. The application of FEM to unbounded domains involves the introduction of artificial boundary conditions to represent the radiation condition [3]; all the available methods provide an approximation of this condition, introducing a further source of inaccuracy. Hybrid methods [4] can be effective in satisfying the radiation condition and controlling the pollution error. In particular, the use of an integral formulation is well-established [5][6] for a quiescent media, even in combination with FEM [7]. For uniform mean flows, an extension of the Kirchhoff's formula is provided by Farassat and Myers [8]. If a radiating surface is used to propagate waves in free field, the acoustic particle velocity has to be accurately predicted by FEM.

We present a hybrid FEM/Radiating-surface approach with a mean flow. The radiating surface formulation is based on the boundary integral formulation developed by Wu and Lee [9]. At the best knowledge of the authors this formulation has yet to be extended to hybrid methods. FEM solves for the scattering problem with a non-uniform mean flow; the radiating surface propagates the acoustic waves in free field by accounting for uniform mean flow effects. The sources of numerical error related to the hybrid method are discussed. The summary of this paper is as follows. Section 2 introduces the physical model. Section 3 presents the coupled FEM/Radiating-surface method; Section 4 describes the numerical sources of error associated to the hybrid method. Finally, numerical examples of the hybrid method are given.

## 2. Governing equations and boundary conditions

We consider wave propagation on a non-uniform mean flow. The acoustic perturbations are assumed of small amplitude; a potential flow is considered such that an acoustic velocity potential  $\phi$  can be introduced. This problem is described in the frequency domain by assuming the implicit time dependence  $e^{i\omega t}$ :

$$(1) \quad \frac{\partial}{\partial t} \left( \frac{\rho_0}{c_0^2} \frac{D_0 \phi}{Dt} \right) - \nabla \cdot \left( \rho_0 \nabla \phi - \frac{\rho_0}{c_0^2} \frac{D_0 \phi}{Dt} \mathbf{u}_0 \right) = 0$$

where  $D_0()/Dt = i\omega() + \mathbf{u}_0 \cdot \nabla()$  indicates the material derivative in the mean flow and  $\partial()/\partial t = i\omega()$ ;  $\rho_0$  is the mean flow density,  $c_0$  the sound speed and  $\mathbf{u}_0$  the mean flow velocity.

Since we deal with an unbounded domain, the Sommerfeld radiation condition is satisfied,

$$(2) \quad \lim_{\|\mathbf{x}\| \rightarrow \infty} \|\mathbf{x}\| \left( (\mathbf{u}_\infty \cdot \mathbf{n} + c_0) \frac{\partial}{\partial \|\mathbf{x}\|} + ik \right) \phi = 0$$

with the wavenumber  $k = \omega/c_0$ ,  $\mathbf{n}$  the outgoing normal vector to the domain and  $\mathbf{u}_\infty$  the uniform mean flow velocity. The problem is solved for Neumann boundary conditions by assuming rigid body scattering:

$$(3) \quad \frac{\partial \phi}{\partial n} = 0 \quad \text{on } \Gamma$$

where  $\Gamma \in \partial\Omega$  is the scattering surface. Equation (3) represents the zero acoustic velocity at the scatterer surface, namely,  $\nabla \phi \cdot \mathbf{n} = \mathbf{u} = 0$ .

## 3. Numerical method

The weak variational formulation for the full potential equation is reviewed. In the FEM formulation, a Perfectly Matched Layer (PML) is used to represent the radiation condition; an integral formulation with a uniform mean flow is used for noise propagation in free field. The coupled FEM/Radiating-surface formulation includes mean flow effects.

### 3.1 Weak variational formulation

The physical model in Eq. (1) is reformulated by introducing a weak variational statement. This formulation minimises the error on the residuals of the formulation. A double integration by parts of the integral equation projected on a test function is performed. The test function  $w$  is introduced such that Eq. (1) can be rewritten as:

$$(4) \quad \int_{\Omega} -\frac{\rho_0}{c_0^2} \frac{D_0^* w}{Dt} \frac{D_0 \phi}{Dt} + \rho_0 \nabla w^* \cdot \nabla \phi dV = \int_{\Gamma} \left[ -\frac{\rho_0}{c_0^2} w^* \frac{D_0 \phi}{Dt} (\mathbf{u}_0 \cdot \mathbf{n}) + \rho_0 w^* \nabla \phi \cdot \mathbf{n} \right] d\Gamma$$

where the superscript "\*" indicates the complex conjugate.

The linear system of equations associated to FEM is based on Eq. (4); we consider a first order polynomial interpolation in the discrete formulation. This approximation requires a high level of refinement to limit the discretisation and pollution errors, though the condition number is better than for a high-order interpolation basis. The radiation condition is modelled by using a Perfectly Matched Layer (PML) [10]. The extended domain absorbs the incoming waves avoiding reflections at the outer boundary of the domain. Following Bermudez et al. [11], we use logarithmic stretching functions for the PML implementation. In the non-physical domain, the problem is formally equivalent to Eq. (4) but it accounts for the space transformation based on the stretching functions.

### 3.2 Radiating surface

An acoustic field embedded in a closed surface can be represented by an equivalent field radiated by the envelope. The Kirchhoff-Helmholtz's surface integral [5] is extended to the case of uniform mean flows on the basis of the boundary integral formulation derived by Wu [9]. The acoustic potential in any point external to the radiating surface is:

$$(5) \quad \phi(\zeta) = \int_{\Gamma_{cs}} \frac{\partial \phi(\boldsymbol{\eta})}{\partial n_{\boldsymbol{\eta}}} G_a(\zeta, \boldsymbol{\eta}) - \phi(\boldsymbol{\eta}) \frac{\partial G_a(\zeta, \boldsymbol{\eta})}{\partial n_{\boldsymbol{\eta}}} - 2ikM_{\infty} G_a(\zeta, \boldsymbol{\eta}) \phi(\boldsymbol{\eta}) n_{\boldsymbol{\eta},x} - M_{\infty}^2 \left( G_a(\zeta, \boldsymbol{\eta}) \frac{\partial \phi(\boldsymbol{\eta})}{\partial x} - \phi(\boldsymbol{\eta}) \frac{\partial G_a(\zeta, \boldsymbol{\eta})}{\partial x} \right) n_{\boldsymbol{\eta},x} d\Gamma$$

where  $G_a(\zeta, \boldsymbol{\eta})$  is the Green's function associated to the adjoint operator of the convected Helmholtz equation and  $\Gamma_{cs}$  is the closed control surface;  $\mathbf{n}_{\boldsymbol{\eta}}$  is the unit normal vector pointing outside the physical domain,  $\phi(\boldsymbol{\eta})$  the potential at the coupling surface and  $\frac{\partial \phi(\boldsymbol{\eta})}{\partial n_{\boldsymbol{\eta}}}$  the related normal component of the gradient. The component of the normal vector to the boundary surface in the direction of the  $x$ -axis is  $n_{\boldsymbol{\eta},x}$  and  $M_{\infty}$  is the uniform flow Mach number. The vector  $\zeta$  indicates a field point external to the radiating surface, whereas  $\boldsymbol{\eta}$  points to the Kirchhoff's surface. For clarity, we assume the flow aligned with the positive  $x$ -axis.

The integral over the control surface is nothing but the integral over a combination of equivalent monopole and dipole sources; a generic acoustic field is replaced by an equivalent distribution of elementary sources. In other words, if the distribution of pressure and velocity is known on the closed permeable surface it is possible to predict the field in every point external to the envelope. The formulation reduces to the canonic Kirchhoff's integral for  $M_{\infty} \rightarrow 0$ .

Since we are solving the problem of radiation in free field, the solution of the fundamental adjoint operator of the convected Helmholtz equation is obtained by reversing the direction of the flow in the Green's function associated to the fundamental operator. We consider the wave propagation on a subsonic mean flow. For 3D problems [9],

$$(6) \quad G_a(\boldsymbol{\eta}, \boldsymbol{\eta}_s) = \frac{e^{-ik \frac{R_M + M_{\infty}(\boldsymbol{\eta}_x - \boldsymbol{\eta}_{s,x})}{1 - M_{\infty}^2}}}{4\pi R_M}$$

with  $R_M = \sqrt{(\boldsymbol{\eta}_{,x} - \boldsymbol{\eta}_{s,x})^2 + (1 - M_{\infty}^2)[(\boldsymbol{\eta}_{,y} - \boldsymbol{\eta}_{s,y})^2 + (\boldsymbol{\eta}_{,z} - \boldsymbol{\eta}_{s,z})^2]}$  and  $\boldsymbol{\eta}_s$  the location vector of the source; for 2D problems [12],

$$(7) \quad G_a(\boldsymbol{\eta}, \boldsymbol{\eta}_s) = -\frac{i}{4\sqrt{1 - M_{\infty}^2}} H_0^{(2)} \left( \frac{kR_N}{1 - M_{\infty}^2} \right) e^{-i \frac{M_{\infty}}{1 - M_{\infty}^2} k(\boldsymbol{\eta}_x - \boldsymbol{\eta}_{s,x})}$$

with  $R_N = \sqrt{(\boldsymbol{\eta}_{,x} - \boldsymbol{\eta}_{s,x})^2 + (1 - M_{\infty}^2)(\boldsymbol{\eta}_{,y} - \boldsymbol{\eta}_{s,y})^2}$  and  $H_0^{(2)}$  the Hankel function of the second kind of order zero. The above Green's functions satisfy the Sommerfeld radiation condition.

### 3.3 Coupled solution

This section presents the procedure by which the FEM solution is coupled with the integral formulation. By using FEM, the sound field is computed in the region where the scattering occurs in presence of a non-uniform flow and the solution is mapped on a closed surface where the mean flow is uniform. Noise is radiated by means of the integral formulation in Eq. (5).

The scattering problem is solved by using Eq. (4) associated with a polynomial expansion of the solution. The use of FEM leads to a linear system of equations:

$$(8) \quad \mathbf{K}_{AP} \mathbf{s} = \mathbf{f}$$

where  $\mathbf{K}_{AP}$  is the matrix of the coefficients obtained by the discrete formulation of the domain integral in Eq. (4) and  $\mathbf{f}$  accounts for the integral on the boundary and any distribution of sources in the domain;  $\mathbf{s}$  is the vector of the nodal Degrees of Freedom (DoFs): it accounts for all the internal and boundary nodal values of the acoustic potential, i.e.,  $\mathbf{s} = [\phi_1, \phi_2, \dots, \phi_N]$ . The PML is applied at the outer boundary of the FEM domain.

The solution of the problem is physical in the whole domain except for the PML region. In the physical domain, any closed surface can be used as a radiating surface. If the FEM solution at the permeable surface is indicated by  $\phi_{FEM}$ , Eq. (5) can be expressed as,

$$(9) \quad \phi(\boldsymbol{\zeta}) = \int_{\Gamma_{cs}} \frac{\partial \phi_{FEM}(\boldsymbol{\eta})}{\partial n_{\boldsymbol{\eta}}} G_a(\boldsymbol{\zeta}, \boldsymbol{\eta}) - \phi_{FEM}(\boldsymbol{\eta}) \frac{\partial G_a(\boldsymbol{\zeta}, \boldsymbol{\eta})}{\partial n_{\boldsymbol{\eta}}} - 2ikM_{\infty} G_a(\boldsymbol{\zeta}, \boldsymbol{\eta}) \phi_{FEM}(\boldsymbol{\eta}) n_{\boldsymbol{\eta},x} - M_{\infty}^2 \left( G_a(\boldsymbol{\zeta}, \boldsymbol{\eta}) \frac{\partial \phi_{FEM}(\boldsymbol{\eta})}{\partial x} - \phi_{FEM}(\boldsymbol{\eta}) \frac{\partial G_a(\boldsymbol{\zeta}, \boldsymbol{\eta})}{\partial x} \right) n_{\boldsymbol{\eta},x} d\Gamma$$

Since the FEM solution is computed at the nodal points and eventually mapped on the closed surface, the formulation can be discretised by using linear interpolating functions; for Lagrangian formulations, a high order interpolation is necessary to preserve the FEM accuracy. In fact, the only physical information is provided by the DoFs solved by FEM at the nodal points. Therefore, we assume that

$$(10) \quad \begin{aligned} \phi_{FEM}(\mathbf{x}) &\simeq \sum_l^M N_l(\mathbf{x}) \phi_l^- \\ \nabla \phi_{FEM}(\mathbf{x}) &\simeq \sum_l^M N_l(\mathbf{x}) \nabla \phi_l^- \end{aligned}$$

where  $N_l(\mathbf{x})$  is the  $l$ -th shape function;  $\phi_l^-$  and  $\nabla \phi_l^-$  are computed by FEM on the radiating surface. In a generic point external to the radiating surface, the solution is given by introducing the above polynomial expansion into Eq. (9). This leads to:

$$(11) \quad \phi(\boldsymbol{\zeta}) = \mathbf{A} \boldsymbol{\phi}^- + \mathbf{B} \frac{\partial \boldsymbol{\phi}^-}{\partial \mathbf{n}} + \mathbf{C} \frac{\partial \boldsymbol{\phi}^-}{\partial \mathbf{x}};$$

the adjoint Green's function is well-known, the coefficient of the matrices  $\mathbf{A}$ ,  $\mathbf{B}$  and  $\mathbf{C}$  are computed, whereas the vectors  $\boldsymbol{\phi}^-$ ,  $\frac{\partial \boldsymbol{\phi}^-}{\partial \mathbf{n}}$  and  $\frac{\partial \boldsymbol{\phi}^-}{\partial \mathbf{x}}$  are given by FEM. Since Eq. (5) is exact only for a uniform mean flow, the two methods can be coupled only in a region where this condition is fulfilled.

## 4. Error analysis

### 4.1 Error estimates

The numerical error for the hybrid FEM/Radiating-surface approach is described. The FEM solution introduces both discretisation and dispersion errors; the build-up of the dispersion error is

addressed as pollution error. The convection effect due to the mean flow increases the pollution error [2]. On the other hand, the integral formulation in Eq. (5) is infinitely accurate; in this case, the sources of numerical error are the discretisation of the radiating surface and the accuracy of the quantities mapped on it. The Kirchhoff's integral is not affected by pollution error.

For the  $hp$ -FEM, the  $H^1$  norm of the numerical error is estimated by Inhlenburg and Babuška [13]:

$$(12) \quad E \leq C_1 \left( \frac{kh}{2P} \right)^P + C_2 k \left( \frac{kh}{2P} \right)^{2P} ;$$

$P$  is the polynomial order of interpolation,  $C_1$  and  $C_2$  are two constants and  $E$  represents the asymptotic behaviour of the error for  $kh \rightarrow 0$ . Equation (12) is applicable to a generic grid pattern: the first term on the r.h.s. is the discretisation error; it is independent of the mean flow if the discretisation is based on  $k = \omega/c_0(1 + M)$ . The second term is the pollution error and it is dependent on the mean flow [2]:  $C_2$  is a function of the length of the domain and the Mach number  $M$ ; it scales with  $(1 - M)$ . For short wavelengths the contribution of the second term becomes significant.

Despite of the accuracy of the quantities mapped on the radiating surface, the numerical error introduced by the integral formulation depends on the surface discretisation. At the nodal points, acoustic pressure and velocity are predicted by FEM and interpolated by means of a polynomial expansion to solve the integral equation Eq. (9). A linear interpolation is performed if the solutions at the nodal points are mapped for linear FEM or  $p$ -FEM. For a Lagrangian formulation, the use of a coherent basis of functions both for FEM and the integral formulation preserves the accuracy of the prediction. A conformal mesh is advisable, even though the FEM solution can be interpolated; for a non-conformal mesh, a loss in accuracy is introduced by mapping the solution.

The use of  $\nabla\phi$  in Eq. (9) can be critical for the formulation. The discrete system of equations related to Eq. (4) solves for the basic variable  $\phi$ . The computation of the related gradient is performed a posteriori: the accuracy of the gradient is one order of polynomial degree lower than the accuracy achieved for  $\phi$ . Therefore, if the level of refinement or the order of interpolation for FEM is inaccurate to compute correctly the acoustic particle velocity, the prediction of the hybrid method might be affected by a large error; this error can cancel any beneficial effect given by the hybrid method.

## 4.2 Discussion of the results

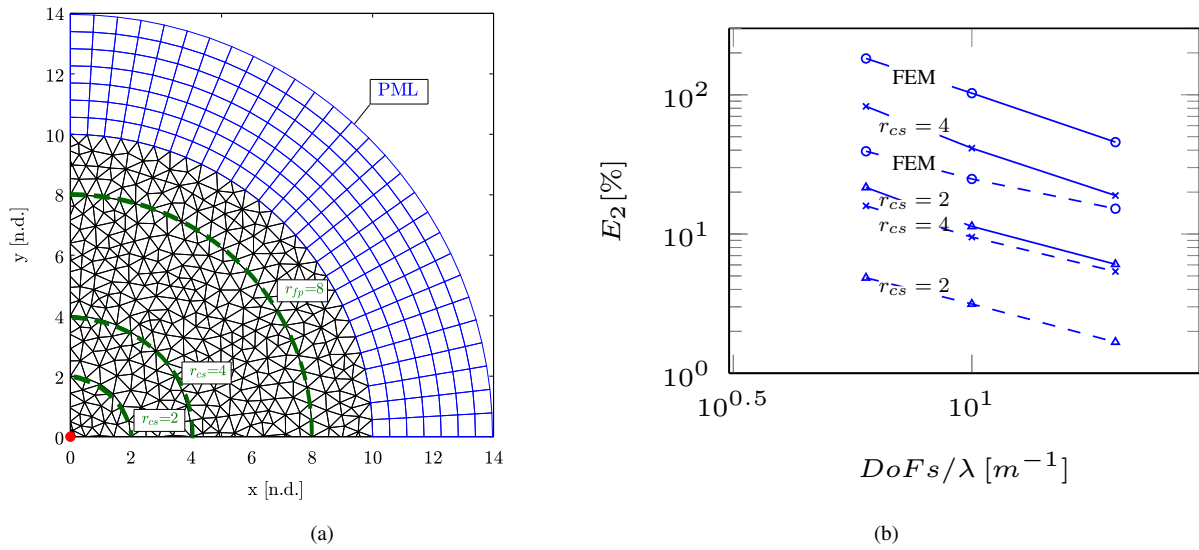
In this section, two test cases are presented to assess the limitations of the hybrid method. First, the radiation of a monopole is discussed; then, the problem of scattering by a cylinder from a monopole source is described. Both problems are solved in 2D. In the case of radiation from a monopole source, the accuracy is assessed against the analytical solution [12]; for the scattering by a cylinder, Morris [14] provides an analytical solution for quiescent media. We use a FEM model with a highly refined grid to compute the reference solution in the case of a non-uniform mean flow. An incompressible steady potential formulation is used to predict the mean flow around the cylinder. We deal with subsonic base flows. For the problems analysed, the reference unit length is the diameter of the cylinder  $d = 2a = 1$ . The error is computed on a field point circumference centered at the origin of the reference frame and with radius  $r_{fp} = 8$ . The problem is analysed by considering two different radiating surfaces, centered at the origin of the coordinate system, with radius  $r_{cs} = 2$  and  $r_{cs} = 4$ . We consider the discrete model for a number of DoFs per wavelength equal to 6, 10, 20.

The FEM solution is based on a first order formulation and an unstructured grid. Although we are aware of the inaccuracy related to the representation of the monopole in FEM, a point source is adopted; the objective is to test the combined approach independently of the source model. The speed of sound is assumed constant  $c_0 = 340 \text{ m/s}$  and the density of the air is  $\rho_0 = 1.2 \text{ kg/m}^3$ . We define a conformal grid where the nodal points of the radiating surface are coincident with the nodes of the FEM grid.

#### 4.2.1 Monopole in free field

A monopole source is defined at the center of the reference frame. The radiating surfaces and the monopole are centered at the origin of the coordinate system. When a uniform flow is accounted for, it is aligned with the positive  $x$ -axis. The error is computed against the analytical solution [12].

Figure 1(a) shows a quarter of the domain of computation for  $kd = 1.85$  and  $6 \text{ DoFs}/\lambda$ , with  $\lambda$  the nominal wavelength. Figure 1(b) depicts the  $L_2$  error for the full FEM solution and the hybrid method for  $r_{cs} = 2$  and  $r_{cs} = 4$ ; the solution is provided for  $kd = 1.85$  and  $kd = 9.24$  at  $M_\infty = 0$ . The results about the convergence follow the well-known P+1 rate, but a factor  $C = 2^{(r_{fp}-r_{cs})/2}$  is scaling the magnitude of the error: the effect of the pollution error is limited by using the radiating surface; particularly, in Eq. (12) the effect of the second term on the r.h.s. is healed by applying the Kirchhoff's surface integral.



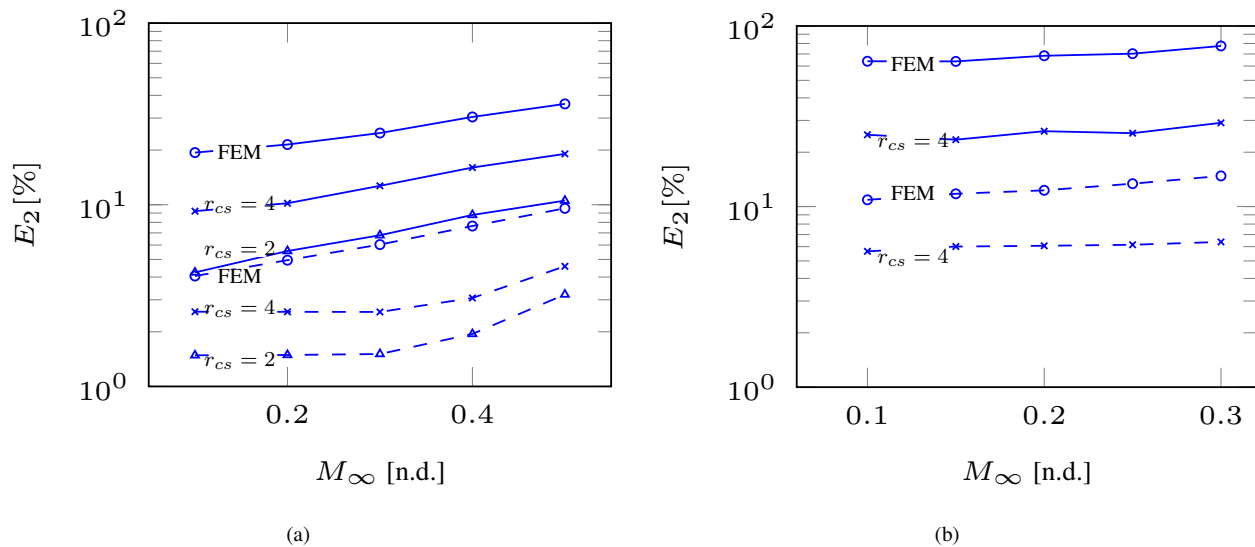
**Figure 1.** (a) Mesh,  $kd = 1.85$  and  $6 \text{ DoFs}/\lambda$ . (b) Convergence analysis: hybrid method vs. full FEM -  $L_2$  error over the analytical solution; Solid lines:  $kd = 9.24$  - Dashed lines:  $kd = 1.85$ . Radiation from a monopole source at  $M_\infty = 0$ .

Figure 2(a) depicts the  $L_2$  error for a number of  $M_\infty$  in the case of radiation from a monopole in free field. We compare the results of the full FEM approach and the hybrid method by accounting for the radiating surfaces with  $r_{cs} = 2$  and  $r_{cs} = 4$  at  $kd = 1.85$  and  $kd = 9.24$ ;  $20 \text{ DoFs}/\lambda$  are used for the FEM solution. The error in the FEM solution increases with  $M_\infty$ : the flow convection introduces a shortening of the wavelength upstream which increases the pollution error. The hybrid method limits this effect: in the worst case scenario for  $r_{cs} = 2$ , the error produced by the coupled solution is half of the error given by the full FEM solution. The plateau observed at  $kd = 1.85$  for low Mach numbers is attributed to the numerical error associated to the source model used for FEM.

#### 4.2.2 Scattering by a cylinder from a monopole source

The scattering by a cylinder from a monopole source is considered. A linear FEM solution accounting for  $30 \text{ DoFs}/\lambda$  is adopted as the reference solution in the case of a non-uniform mean flow. The cylinder has a radius  $a = 0.5$  and it is centered at the origin of the reference frame; the source is located below the cylinder at  $\mathbf{x}_s = [0, -1]$ .

Figure 3(a) shows the domain of computation for  $kd = 1.85$  and  $6 \text{ DoFs}/\lambda$ . Figure 3(b) depicts the  $L_2$  error for the solutions provided by a full FEM approach and the hybrid method for  $r_{cs} = 2$  and  $r_{cs} = 4$ ; the solution is given at  $kd = 1.85$  and  $kd = 9.24$ . The rate of convergence is P+1, and the reduction of the error associated to the hybrid method is frequency related: wave scattering



**Figure 2.** (a) Radiation from a monopole in a uniform flow - 20  $DoFs/\lambda$ ; (b) Scattering by a cylinder from a monopole with a non-uniform mean flow - 10  $DoFs/\lambda$ . Hybrid method vs. full FEM.  $L_2$  error over the reference solution: analytical solution for (a) and highly resolved FEM for (b); Solid lines:  $kd = 9.24$  - Dashed lines:  $kd = 1.85$ .

affects the local wavelength which, in turn, influences both discretisation and pollution errors. The hybrid method improves the accuracy of the solution with a factor which is frequency dependent: at  $kd = 9.24$  the beneficial effect obtained by the radiating surface is larger than at  $kd = 1.85$ ; in fact, the pollution error depends on the extent of the domain and the wavelength.

Figure 2(b) shows the  $L_2$  error for a number of  $M_\infty$  for the scattering by a cylinder from a monopole source in a non-uniform mean flow. The uniform flow is aligned with the  $x$ -axis. We compare the results of the full FEM solution with the hybrid approach by accounting for a radiating surface with  $r_{cs} = 4$  at  $kd = 1.85$  and  $kd = 9.24$ ; 10  $DoFs/\lambda$  are used for FEM. The coupling is performed only at  $r_{cs} = 4$  where the mean flow is uniform. As mentioned for the monopole in free field, the pollution error worsens with the increase of  $M_\infty$ . The linear dependence of the error on the Mach number is retrieved; the error provided by the combined FEM/Radiating-surface approach is half of the error shown by the full FEM solution.

## 5. Conclusion

This paper presents a hybrid FEM/Radiating-surface approach for wave propagation in unbounded domains with a mean flow. The method accounts for a Kirchhoff's integral formulation with a uniform mean flow on the basis of the solution of the adjoint operator for the convected Helmholtz equation. The extent of the FEM domain is conditioned to the definition of the radiating surface, which has to be located in a region where the flow is uniform. The pollution error scales linearly with the Mach number. The hybrid method is effective in limiting the build-up of the dispersion error; this is achieved in presence of a base flow. The effect of the mean flow on the asymptotic behaviour of the dispersion error, for  $kh \rightarrow 0$ , is accounted by considering  $k = \omega/c_0(1 + M)$ . For the hybrid method, a correct prediction of the gradient of the acoustic velocity potential at the radiating surface is necessary to preserve the accuracy of the solution.

## Acknowledgment

The authors gratefully acknowledge the European Commission for funding the project FP7-PEOPLE-2013-ITN CRANE, Grant Agreement 606844.

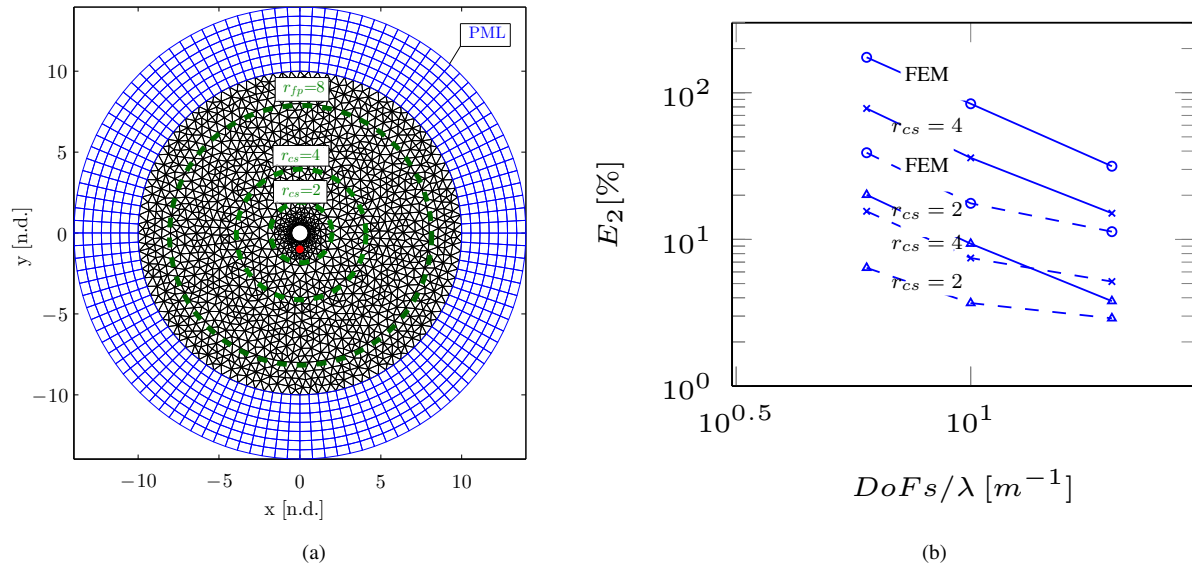


**Figure 3.** (a) Mesh,  $kd = 1.85$ ,  $6 \text{ DoFs}/\lambda$ ; (b) Convergence analysis: hybrid method vs. full FEM.  $L_2$  error over the analytical solution; Solid lines:  $kd = 9.24$  - Dashed lines:  $kd = 1.85$ . Scattering by a cylinder from a monopole source,  $M_\infty = 0$ .

## REFERENCES

1. Babuška, I. and Sauter, S. Is the pollution effect of the FEM avoidable for the Helmholtz equation considering high wave number, *SIAM Journal of Numerical analysis*, **34**, 2392–2423, (1997).
2. Bériot, H., Gabard, G. and Perrey-Debain, E. Analysis of high-order finite elements for convected wave propagation, *International Journal for Numerical Methods in Engineering*, **96**, 655–688, (2013).
3. Astley, R.J. Numerical methods for noise propagation in moving flows, with application to turbofan engines, *Acoustical Science and Technology*, **30** (4), 227–239, (2009).
4. Zienkiewicz, O.C. and et al. *Marriage a la mode - the best of both worlds (finite elements and boundary integrals)*, Wiley, London, Chapter 5, Energy Methods in Finite Elements Analysis, (1979).
5. Ciskowski, R.D. and Brebbia, C.A. *Boundary Element Methods in Acoustics*, Computational Mechanics Publications, Southampton, (1991).
6. Crighton, D.G., Dowling, A.P., Ffowcs Williams, J.E., Heckl, M. and Leppington, F.G. *Modern methods in analytical acoustics*, Springer-Verlag, London, (1992).
7. Bériot, H. and Tournour, M. On the locally-conformal perfectly matched layer implementation for Helmholtz equation, *Proceedings of NOVEN 2009*, Oxford, UK, 5–8 April, (2009).
8. Farassat, F. and Myers, M. K. Extension of the Kirchhoff's formula to radiation from moving surfaces, *Journal of Sound and Vibration*, **123** (3), 451–460, (1988).
9. Wu, T.W. and Lee, L. A direct boundary integral formulation for acoustic radiation in a subsonic uniform flow, *Journal of Sound and Vibration*, **175** (1), 51–63, (1994).
10. Goodrich, J.W. A comparison of three PML treatments for CAA (and CFD), *Proceedings of the 14<sup>th</sup> AIAA/CEAS Aeroacoustics Conference*, Vancouver, British Columbia Canada, 5–7 May, (2008).
11. Bermudez, A., Hervella-Nieto, L., Prieto, A. and Rodriguez, R. An Optimal Perfectly Matched Layer with Unbounded Absorbing Function for Time-Harmonic Acoustic Scattering Problems, *Journal of Computational Physics*, **223** (2), 469–488, (2007).
12. Bailly, C. and Juvé, D. Numerical solution of acoustic propagation problems using linearized Euler equations, *AIAA Journal*, **38** (1), 22–28, (2000).
13. Inhlenburg, F. and Babuška, I. Finite element solution to the Helmholtz equation with high wavenumber. Part II: the hp version of the FEM, *SIAM Journal of Numerical analysis*, **34**, 315–358, (1997).
14. Morris, J. and Brien, O. The scattering of sound from a spatially distributed axisymmetric cylindrical source by a circular cylinder, *Journal of Acoustical Society of America*, **97** (5), 2651–2656, (1994).